Mechanism of air entrainment by a disturbed liquid jet

C. D. Ohl,[a] H. N. Oğuz, and A. Prosperetti[b]
Department of Mechanical Engineering, The Johns Hopkins University, Baltimore, Maryland 21218

(Received 27 April 1999; accepted 7 April 2000)

It was shown in recent work that the crests of surface disturbances on a falling jet are a powerful agent for air entrainment at the free surface of a liquid pool. The paper explores the opposite case in which the jet is disturbed so as to form an axisymmetric trough, rather than a crest. It is found that no air is entrained in this case. The paper concludes with some considerations on the validity of a recently proposed model for air entrainment. © *2000 American Institute of Physics.* [S1070-6631(00)02507-1]

I. INTRODUCTION

Consider a liquid jet falling into a pool of an otherwise quiescent liquid. If precautions are taken to condition the flow so that the jet surface is smooth, one can avoid air entrainment up to Reynolds numbers well beyond 10 000. However, surface disturbances on the jet surface are readily seen to cause entrainment. An example is shown in Fig. 1, where the bulge of liquid falling with the jet is created by rapidly increasing the jet flow rate. In a recent paper in which we have studied this process, we argued that the phenomenon is due to the high stagnation pressure acting on the pool liquid when its surface is struck by the bulge.[1] This momentary high pressure causes the formation of a cavity that collapses from the sides and entraps air as Fig. 1 demonstrates.

The role played by the stagnation pressure can be further examined by considering the converse situation in which the disturbance on the jet surface has the form of an axisymmetric trough, rather than a crest (Fig. 2). The apparatus we used in our earlier study can be easily modified to produce this situation, and we present here some results of this experiment. It is found that in this case the phenomenon is much milder and no entrainment is observed. At the end of the paper we discuss a recent model for air entrainment,[2,3] that was proposed to explain the aeration of the liquid slugs that separate the large bubbles (the so-called Taylor bubbles) encountered in gas–liquid flows in the slug-flow regime.

II. EXPERIMENT

The apparatus is a slight modification of the one described in Ref. 1. In that study, a rapid increase of the jet flow rate was obtained by simultaneously opening four solenoid valves connected to a high-pressure liquid reservoir upstream of the jet exit. For the purposes of the present experiment the valves were instead connected to a low-pressure reservoir that caused a decrease of the jet flow when opened. Pictures of the stroboscopically illuminated jet were taken with a CCD camera (Kodak DC210+). Due to the high reproducibility of the process, by varying the delay between the opening of the valves and the time of illumination, it was possible to capture the temporal evolution of the jet shape.

The velocity U_0 of the undisturbed jet at the nozzle exit was obtained from the flow rate Q_0 measured with a rotameter (OMEGA FL 4503-V) and the nozzle diameter $D_j=5.4$ mm. Upon opening of the valves, the velocity decreases from U_0 to U_1 according to a relation of the type $U(t)=U_0+(U_1-U_0)f(t)$. The function $f(t)$ was measured in Ref. 1 and found to be accurately represented by

$$f(t)=\exp\left[-10\left(\frac{t}{T}-1\right)^2\right], \tag{1}$$

in the range $0\leqslant t\leqslant T$, where $T=13$ ms is the response time of the system. The steady velocity U_1 reached after the opening of the valves was obtained by measuring the volume V_{out} of the liquid flowing into the low-pressure reservoir during the time Δt the valves remain open:

$$U_1=\frac{4}{\pi D_j^2}(Q_0-Q_{\text{out}}). \tag{2}$$

The flow rate Q_{out} into the reservoir is approximated as $Q_{\text{out}}\simeq V_{\text{out}}/\Delta t$, which is sufficiently accurate since $\Delta t\simeq 200$ ms is much longer than the valve response time T.

III. MODEL

In Ref. 1 a quasi-one-dimensional model[4–6] was used to calculate the shape of the jet free surface. The same model is appropriate for the present case. The jet is assumed to be axisymmetric. The z coordinate is vertical and positive downward; $z=0$ corresponds to the nozzle exit. Upon integrating over the jet cross section, the equation of continuity becomes

$$\frac{\partial A}{\partial t}+\frac{\partial}{\partial z}(Au)=0, \tag{3}$$

where $A=A(z,t)$ is the local cross-sectional area of the jet and $u(z,t)$ is the jet velocity (positive downward) averaged over the cross section.

The momentum equation is

[a]Present address: Department of Applied Physics, University of Twente, AE 7500 Enschede, The Netherlands.
[b]Also at: Department of Applied Physics, Twente Institute of Mechanics, and Burgerscentrum, University of Twente, AE 7500 Enschede, The Netherlands. Electronic mail: prosper@jhu.edu

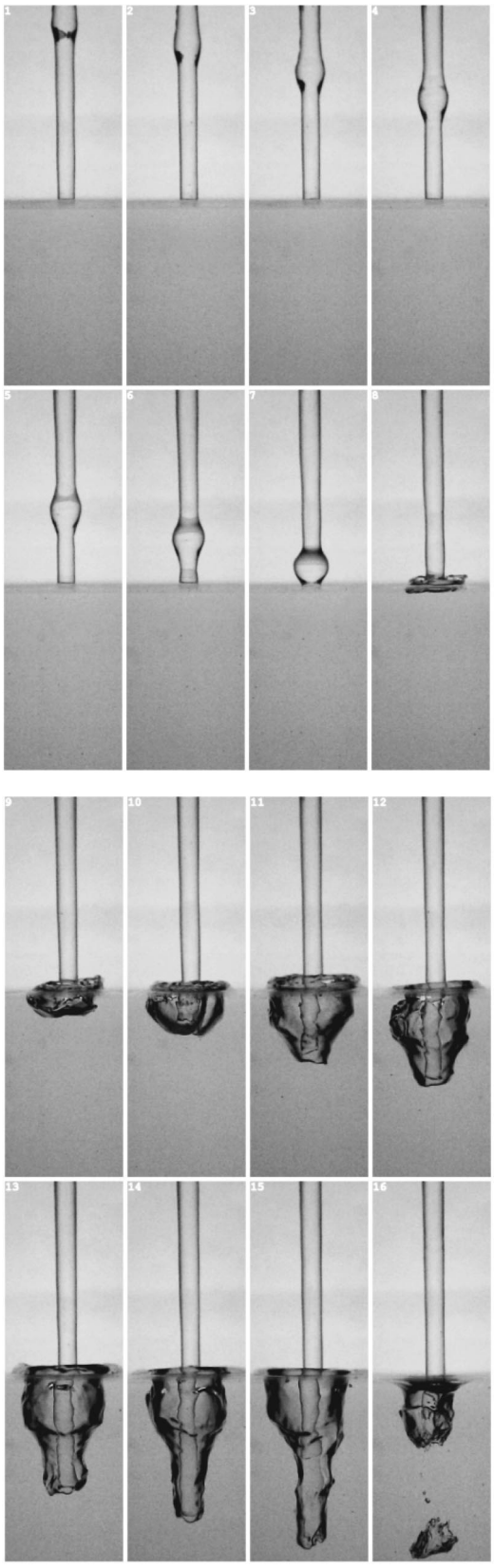

FIG. 1. The sequence of events leading to air entrapment by a disturbance on a falling water jet. The bulge on the jet is caused by a rapid increase of the jet flow rate from 0.98 to 1.35 m/s over a time of about 13 ms. The nozzle diameter is 5.4 mm and its distance from the undisturbed free surface 53 mm. The time interval between successive frames is 5 ms. The field of view in air is 30.0 by 96.4 mm.

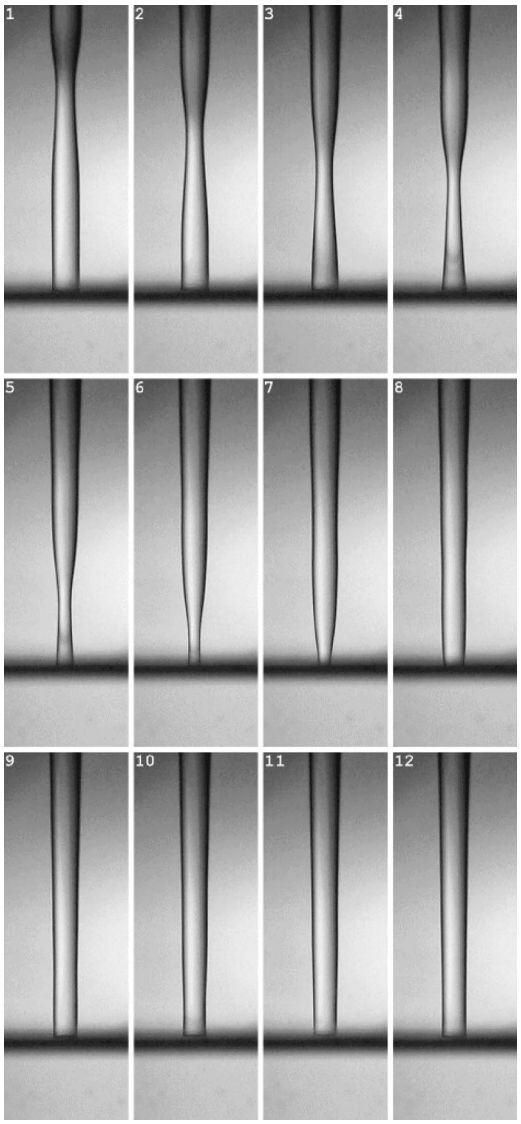

FIG. 2. Evolution of the jet surface after opening the valves that decrease the velocity from 0.98 to 0.66 m/s. Successive frames are separated by 5 ms. The field of view in air is 27.8 by 83.0 mm.

$$\frac{\partial u}{\partial t}+u\frac{\partial u}{\partial z}=g-\frac{1}{\rho}\frac{\partial p}{\partial z}, \tag{4}$$

where the average of u^2 has been approximated by the square of u. This is a good approximation because, due to the thinning of the viscous boundary layer in the contracting part of the nozzle and to the presence of the free surface, the velocity distribution is close to uniform over the jet cross section. Because of the thinness of the jet, the pressure p can be taken to be uniform over the cross section, which leads to the relation

$$p = p_0+\sigma \mathcal{C}, \tag{5}$$

where p_0 is the ambient pressure outside the jet, σ the surface tension coefficient, and $\mathcal{C}$ the local curvature of the interface. We assume that, before opening the valves, the jet is steady and in free fall. Thus, the initial velocity distribution

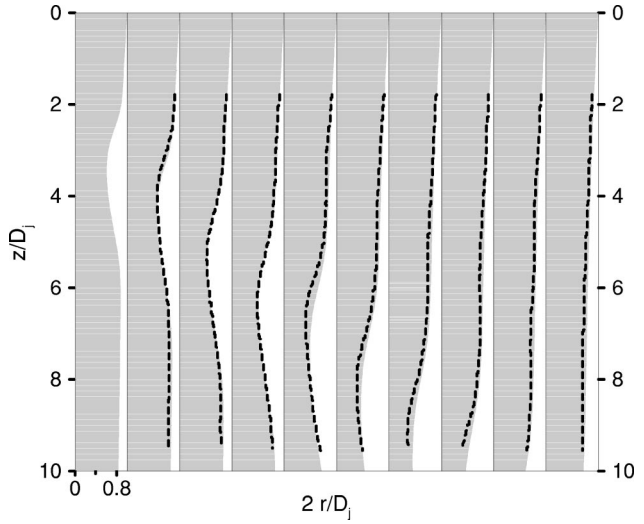

FIG. 3. Comparison of the experimental shapes of the jet surface at different instants of time (dotted lines) with the calculated profiles (shaded areas). The first frame depicts the calculated jet shape 30.5 ms after the opening of the valve; subsequent frames are at 5 ms intervals.

is $u(z,0)=(U_0^2+2gz)^{1/2}$. As a consequence of the mass conservation equation (3) with $\partial A/\partial t=0$, this relation gives the initial jet shape $A(z,0)$.

Equations (3) and (4) are solved numerically by finite differences using a Lax–Wendroff two-step scheme and a Lax scheme, respectively, for time advancement.[7]

IV. RESULTS

Figure 2 is a sequence of photographs separated by 5 ms. Although, as explained before, each photo corresponds to a different event, due to the high reproducibility of the experiment the sequence can be considered a faithful depiction of an individual run. The dark fuzzy horizontal stripe in the lower part of each frame is the meniscus of the pool liquid on the wall of the container. This area separates the air above from the water below. The flow rate at the nozzle exit is $U_0=0.98$ m/s, and the flow rate after opening the valves is $U_1=0.65$ m/s, so that $U_1/U_0=0.66$. Although it would be desirable to generate a stronger disturbance on the jet surface, we were unable to do so as attempts to reduce the velocity any further led to a break-up of the jet. The pool surface is at a distance $z=53$ mm (i.e., 9.8 jet diameters) from the nozzle. It is seen here that, contrary to Fig. 1, the jet disturbance causes no air entrainment.

Figure 3 compares the experimental jet shape with that calculated according to the previous model (dashed line). The shape of the jet surface is extracted from the photographs by means of an edge-detection algorithm based on the local maxima of the gradient of the smoothed image.[8] In the calculations we used $\rho=998.2\,\mathrm{kg/m^3}$ for the liquid density, $\sigma=0.072\,75\,\mathrm{N/m}$ for the surface tension, and $g=9.81\,\mathrm{m/s^2}$ for the acceleration of gravity.

Overall, the agreement between the experiment and the quasi-one-dimensional model is very good. Some differences are encountered only in regions of strong curvature, e.g., the fifth frame of Fig. 3. As in Ref. 1, the model tends to underestimate the curvature in these conditions.

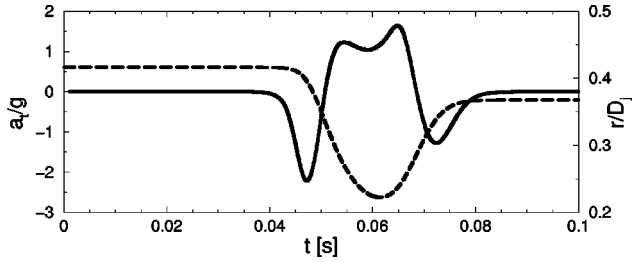

FIG. 4. Normalized horizontal acceleration a/g (negative inward, solid curve) of the contact line between the jet and the pool liquid and normalized jet radius R/D_j (dashed line, right vertical scale).

From these theoretical results we can calculate the acceleration with which the contact line between the jet and the pool liquid moves in the horizontal plane. These results are shown in Fig. 4 for the case of Figs. 2 and 3. Here the solid line is the apparent horizontal acceleration of the contact line at the level of the free surface of the pool liquid and the dashed line is the jet radius R (to be read on the right vertical scale). As the jet diameter decreases, the acceleration falls below $-2g$ while it reaches nearly $2g$ in the opposite direction as the jet diameter recovers. Since, as noted before, the model tends to underestimate the jet curvature, the actual acceleration is probably somewhat more negative than the estimated model value.

It is also interesting to present a different view of the surface disturbance of the pool liquid, which is given in Fig. 5. Here the individual photographs are taken for the same experimental parameters as in Fig. 2 and correspond to the same instants of time, but the camera is set at an angle so as to capture the pool surface together with the jet shape. As the jet disturbance approaches the pool (frame 5 of Fig. 5), a depression forms on the surface. This depression reaches its maximum at about the time the thinnest part of the jet

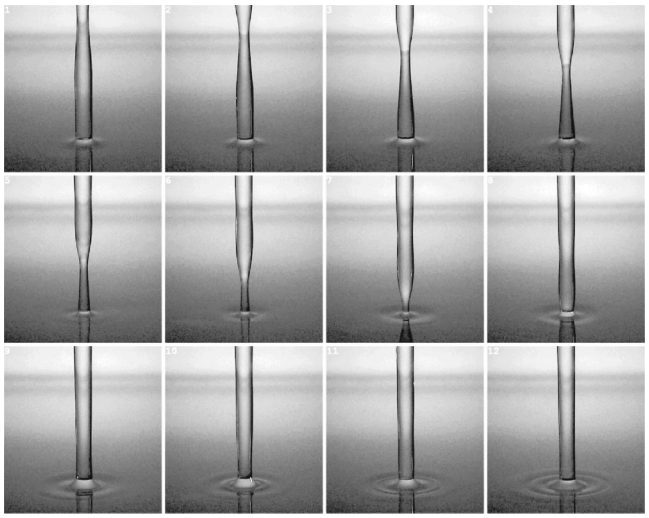

FIG. 5. Oblique view of the same event shown in Fig. 2 looking down toward the pool surface. Note the depression formed by the thinning of the local diameter, followed by the generation of capillary waves when the normal diameter is restored.

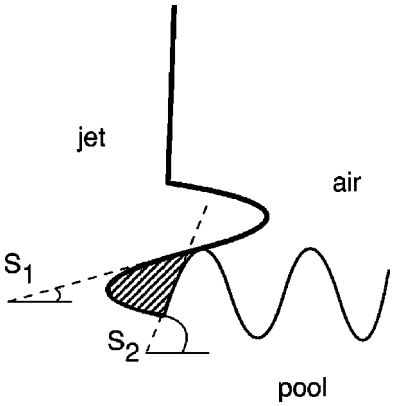

FIG. 6. Sketch of the air entrapment mechanism proposed in Refs. 2 and 3. It is postulated that surface disturbances on the jet surface entrap air (shaded area) by a ''capping'' action.

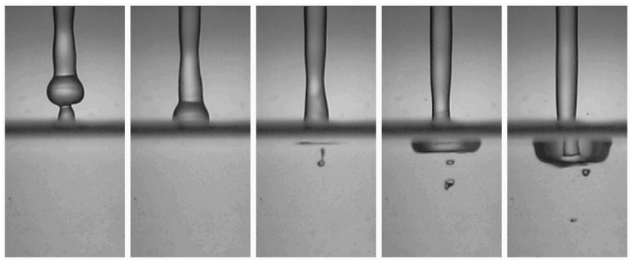

FIG. 7. The bulge shown here is generated by increasing the jet velocity from 0.69 to 1.06 m/s and is, therefore, bigger than that of Fig. 1. As a consequence, the outer rim of the bulge bends downward, the criterion (6) is satisfied, and a small bubble is entrapped (frame 3), which subsequently breaks up due to shear (frames 4 and 5). In the last two frames the onset of the large cavity generated by the stagnation pressure is visible. As before, the images in this sequence correspond to different events but the consistent appearance of the small entrapped bubble shows the remarkable detailed reproducibility of the process. The time interval between frames is 5 ms and the field of view in air 28 by 58 mm.

reaches the surface, which happens between frames 7 and 8. The process is similar to a ''rarefaction wave'' on the surface of the pool liquid. At later times, as the jet diameter recovers, circular capillary waves are seen to radiate away from the impingement point.

V. DISCUSSION

In recent work on air entrainment in gas–liquid slug flow,[2,3] an essentially geometric criterion for air entrainment was proposed. The postulated mechanism is shown in Fig. 6 and the condition for entrainment is phrased in terms of the two slopes S_1, S_2 shown in the figure as

$$S_2 > S_1. \tag{6}$$

The authors assume that a series of surface waves is present on both the vertical and the horizontal liquid surfaces and further elaborate this condition formulating it in terms of wavelengths and wave amplitudes. Since in our case we only have a single disturbance on the jet, and no waves on the pool surface (at least initially), it is best to consider the entrainment criterion in the original form (6), rather than in the derived form based on a conceptual picture not directly applicable to our situation. It may be noted that a similar geometric picture of air entrainment has been considered before (see e.g., Ref. 9 cited in Ref. 10 and Refs. 11 and 12) and successfully used, in a slightly different context, in Ref. 13.

Let us first consider the case of a ''negative'' bulge shown in Figs. 2 and 5. In this case the pool surface perturbation is very mild so that $S_2 \simeq 0$ while, after the passage of the point of minimum diameter, S_1 is relatively close to $\frac{1}{2}\pi$ so that (6) is not satisfied and, indeed, no entrainment is observed.

It would be hard, however, to explain air entrainment in the case of a positive bulge on the basis of the criterion (6). After striking the water surface, not only Fig. 1, but all our other pictures (some of which were published in Ref. 1) clearly show that the bulge loses its integrity and the jet surface in the developing cavity is smooth, except for the effect of optical distortions due to capillary waves. It is evident from the photos that, after the initial bulge impact, the process of air entrapment is not related in any way to the presence of disturbances on the jet, but is simply the result of the closing of the cavity against the jet surface. The process is, therefore, governed by dynamics rather than geometry as the criterion (6) would imply. We reached the same conclusion in an earlier work[14] devoted to the initial impact of a cylindrical liquid mass on an undisturbed water surface. Also in that case the evolution of the phenomenon is very similar to the present one, with a cavity produced by the large stagnation pressure that eventually collapses on itself entrapping an air bubble. In this case as well the criterion (6) does not apply.

These conclusions of course do not imply that a particular spatial arrangements of the free surfaces coming into contact cannot entrap bubbles. An example is shown in Fig. 7 where a small bubble is caught in the underside of a strong positive bulge similar to that of Fig. 1. Here the pool surface is nearly flat so that $S_2 \simeq 0$, while the lower surface of the bulge bends downward toward the rim, so that $S_1 < 0$ and (6) is satisfied. In frames 3 and 4 of this sequence the entrapped bubble is seen to split in two, probably due to the shear layer between the jet flow and the pool liquid. The early stages of formation of the large cavity produced by the stagnation pressure are visible in the last two frames.

A more dramatic example occurs when the jet surface is very rough as, in these circumstances, the repeated impacts of the surface disturbances give rise (on average) to an air sheath separating the jet from the pool liquid.[9–12,15,16] In these conditions, the crest of a wave on the surface of the falling liquid often entraps an air mass by ''capping'' a surface depression as postulated in Refs. 2, 3, and 17. (This situation is different from that encountered at low Reynolds numbers, where the air sheath is nearly steady and is caused by viscous effects.[18] Under these circumstances, air entrainment probably occurs through an instability of the air film as hypothesized in Ref. 19.) Thus, while the model (6) does not fit the present observations, it is certainly applicable in other conditions. The point we wish to stress, however, is that the degree of surface disruption necessary for the criterion (6) to lead to air entrapment is only possible under the action of the

powerful stagnation pressures caused by the repeated impact of positive (outward) surface disturbances.

ACKNOWLEDGMENTS

The authors express their appreciation to the authors of Refs. 2, 3, and 17 for sharing with them their data prior to publication and for motivating this work. This study has been supported by the Office of Naval Research.

[1]Y. G. Zhu, H. N. Oğuz, and A. Prosperetti, ''Air entrainment by impinging liquid jets with surface disturbances,'' J. Fluid Mech. **404**, 151 (2000); see also Phys. Fluids **10**, S3 (1998).
[2]J. Kockx, ''Experiments on the gas exchange between a Taylor bubble and its liquid slug in a vertical tube,'' Ph.D. thesis, Delft University of Technology, Delft, The Netherlands, 1999.
[3]J. P. Kockx, F. T. M. Niewstadt, R. V. A. Oliemans, and R. Delfos, ''Instantaneous film thickness measurements on a Taylor bubble in a vertical tube'' (in preparation).
[4]D. B. Bogy, ''Wave propagation and instability in a circular semi-infinite liquid jet harmonically forced at the nozzle,'' J. Appl. Mech. **45**, 469 (1978).
[5]G. Meier, A. Klöpper, and G. Grabitz, ''The influence of kinematic waves on jet breakdown,'' Exp. Fluids **12**, 173 (1992).
[6]G. Meier, S. Loose, and B. Stasicki, ''Unsteady liquid jets,'' Appl. Sci. Res. **58**, 207 (1998).
[7]W. H. Press, W. T. Vetterling, S. A. Teukolsky, and B. P. Flannery, *Numerical Recipes in C*, 2nd ed. (Cambridge U.P., Cambridge, 1995).
[8]J. Canny, ''A computational approach to edge detection,'' IEEE Trans. Pattern Anal. Mach. Intell. **8**, 679 (1986).
[9]M. J. McCarthy, J. Henderson, and N. A. Molloy, ''Entrainment by plunging jets,'' in *Proc. Chemeca 1970 Conf.* (Butterworths, London, 1970), pp. 86–100.
[10]J. M. Burgess, N. A. Molloy, and M. J. McCarthy, ''A note on the plunging liquid jet reactor,'' Chem. Eng. Sci. **27**, 442 (1972).
[11]D. A. Ervine, E. McKeogh, and E. M. Elsawy, ''Effect of turbulence intensity on the rate of air entrainment by plunging water jets,'' Proc. Inst. Chem. Engrs. **69**, 425 (1980).
[12]A. K. Biń, ''Gas entrainment by plunging liquid jets,'' Chem. Eng. Sci. **48**, 3585 (1993).
[13]H. N. Oğuz, ''The role of surface disturbances in the entrainment of bubbles by a liquid jet,'' J. Fluid Mech. **372**, 189 (1998).
[14]H. N. Oğuz, A. Prosperetti, and A. R. Kolaini, ''Air entrapment by a falling water mass,'' J. Fluid Mech. **294**, 181 (1995).
[15]E. Van de Sande and J. M. Smith, ''Surface entrainment by high-velocity water jets,'' Chem. Eng. Sci. **28**, 1161 (1973).
[16]E. J. McKeogh and D. A. Ervine, ''Air entrainment rate and diffusion pattern of plunging liquid jets,'' Chem. Eng. Sci. **39**, 1161 (1981).
[17]R. Delfos, ''Experiments on air entrainment from a stationary slug bubble in a vertical tube,'' Ph.D. thesis, Delft University of Technology, Delft, The Netherlands, 1996.
[18]T. J. Lin and H. G. Donnelly, ''Gas bubble entrainment by plunging laminar liquid jets,'' AIChE. J. **12**, 563 (1966).
[19]A. M. Lezzi and A. Prosperetti, ''The stability of an air film in a liquid flow,'' J. Fluid Mech. **226**, 319 (1991).